electronics

MDPI

Article

Improved Soft-Starting Method for Doubly Fed Induction Machines Based on Standstill Rotor-Side Synchronization

Kumar Mahtani [1,*], José M. Guerrero [2], José A. Sánchez [3] and Carlos A. Platero [1]

[1] Department of Automation, Electrical and Electronic Engineering and Industrial Informatics, Escuela Técnica Superior de Ingenieros Industriales, Universidad Politécnica de Madrid, 28006 Madrid, Spain; carlosantonio.platero@upm.es
[2] Department of Electrical Engineering, Escuela de Ingeniería de Bilbao, Universidad del País Vasco, 48013 Bilbao, Spain; josemanuel.guerrerog@ehu.eus
[3] Department of Hydraulic, Energy and Environmental Engineering, Escuela Técnica Superior de Ingenieros de Caminos, Canales y Puertos, Universidad Politécnica de Madrid, 28040 Madrid, Spain; joseangel.sanchez@upm.es
* Correspondence: kumar.mahtani@upm.es

Abstract: This paper addresses the challenge of developing a cost-effective and efficient soft-starting method for doubly fed induction machines (DFIMs), a critical requirement for various industrial applications, such as pumped-storage hydropower. The research aims to improve a previously developed starting method by introducing a rotor-side synchronization technique at standstill conditions, which simplifies the starting process and eliminates the need for additional equipment such as autotransformers, resistors, or auxiliary converters. The proposed method begins with the stator winding being fed directly from the power system, while the rotor-side converter adjusts the voltage and frequency to achieve synchronization. Once synchronized, the rotor frequency is gradually reduced by the converter, resulting in a smooth acceleration of the machine. The methodology is validated through a combination of simulations and experimental testing, demonstrating the effectiveness of the proposed approach. The results reveal smooth startup dynamics, with significant reductions in electrical stress, operational complexity, and converter sizing requirements compared to existing methods. Notably, the magnetizing current is supplied directly by the power system through the stator, reducing the burden on the rotor converter by 60% compared to the previous method. The conclusions highlight the method's robustness and its potential as a superior alternative to existing DFIM starting techniques.

Keywords: doubly fed induction generators; hydroelectric power generation; pumped-storage hydropower; renewable energy; starting; synchronization

Academic Editor: Wei Wang

Received: 26 November 2024
Revised: 20 December 2024
Accepted: 24 December 2024
Published: 26 December 2024

Citation: Mahtani, K.; Guerrero, J.M.; Sánchez, J.A.; Platero, C.A. Improved Soft-Starting Method for Doubly Fed Induction Machines Based on Standstill Rotor-Side Synchronization. *Electronics* **2025**, *14*, 48. https://doi.org/10.3390/electronics14010048

1. Introduction

Pumped-storage hydropower systems are among the most efficient and widely implemented methods for large-scale energy storage [1–3], particularly in the context of renewable energy integration [4]. Furthermore, these systems can provide critical services, such as grid balancing, frequency regulation, and peak load management [5,6]. At the heart of these systems lies the energy conversion machinery, which allows to reversibly work in pumping mode (water transfer from the lower reservoir to the upper reservoir) and turbine mode (the opposite) according to the operating requirements. Among the electrical rotating machinery used for this purpose, the induction machine [7], specifically the doubly fed induction machine (DFIM), has gained prominence due to its distinct advantages in variable-speed operation and controllability [8].

The DFIM [9] is suited for variable-speed pumped storage due to its capability to operate efficiently over a broad range of rotational speeds while maintaining precise control of active and reactive power. By interfacing the rotor circuit with a back-to-back converter, the DFIM allows bidirectional power flow and reactive power support, which are essential in both pumping and generating modes. Furthermore, the use of partial-capacity converters—typically 20–30% of the machine's rated power, only rated to provide the slip power—significantly reduces the cost and losses associated with power electronics, compared to fully rated converter-based systems.

A defining characteristic of pumped storage power plants is the operating requirement of transitioning between generating and pumping modes [10]. Generally, when starting the unit in pumping mode, the wicket gates are closed. Then, a depressed tailwater level is achieved through the application of pressurized air to lower the water level at the runner chamber. This dewatering allows for a lower starting torque requirement. This process can take several minutes (5–10 min) [11]. Once completed, the machine is started under no-load conditions. In conventional starting methods, the motor is accelerated up to its operating speed, and then the synchronization with the power system is achieved. The pressurized air is released to allow the filling of the chamber with water, priming the pump. Subsequently, the gates are gradually opened to initiate the pumping process, enabling the transfer of water to the upper reservoir.

Within the process, the starting of the DFIM from standstill to the rated speed is a notable aspect. Effective methods to accelerate the motor for pumping are needed. Most of the existing approaches [12–31] to DFIM starting involve multiple switchgear maneuvers throughout the process, such as stator or rotor short-circuits, or require additional components, such as auxiliary power converters and switches. This poses a technical challenge and impairs the operating efficiency of pumped hydro storage units.

This paper proposes an improvement to a soft start-up approach previously presented by the authors [32], consisting of the stator-side synchronization of the machine with the power system at standstill conditions and subsequent acceleration by rotor voltage and frequency control. In the improved method, the synchronization is proposed on the rotor side, ensuring that the initial current is drawn from the grid by the stator circuit. Therefore, the main contribution of the proposed method compared to the previous method is the avoidance of electrical stress on the converter. This avoidance expands the converter lifespan, from the operational point of view, and allows lower converter sizing requirements, from the system design point of view. Also, pulsed stress on the stator winding before synchronization is an undesirable effect, which is avoided by the proposed approach.

Furthermore, the proposed method eliminates the need for complex maneuvers in the starting process, such as stator or rotor short-circuits, as well as the need for additional equipment for the start-up process, such as autotransformers, resistor, or auxiliary power converters. Consequently, the approach is simpler and more cost-effective than state-of-the-art methods for the same purpose. The method presents smooth starting dynamics, avoiding high inrush currents and voltage sags, and contributing to grid stability.

This paper is structured as follows: Section 2 presents the existing DFIM start-up techniques. Section 3 describes the operating principles of the proposed method. Section 4 reports the results from the computer simulations conducted to verify the operability of the proposed method. Section 5 presents the experimental results conducted on a grid-connected testbench comprising a 7.5 kW DFIM. Based on the results, Section 6 provides a discussion comparing the proposed method with other techniques, highlighting the contributions of the present work. Finally, Section 7 closes the paper, summarizing the main points and opening avenues for future work.

2. State of the Art

The existing methods for DFIM starting have been divided into three main categories: opposite-phase sequence-based methods, reduced voltage-based methods, and auxiliary converter-based methods. In the following, each category will be described, pointing out their technical advantages and drawbacks. The electrical schemes for each type of method are illustrated in Figure 1.

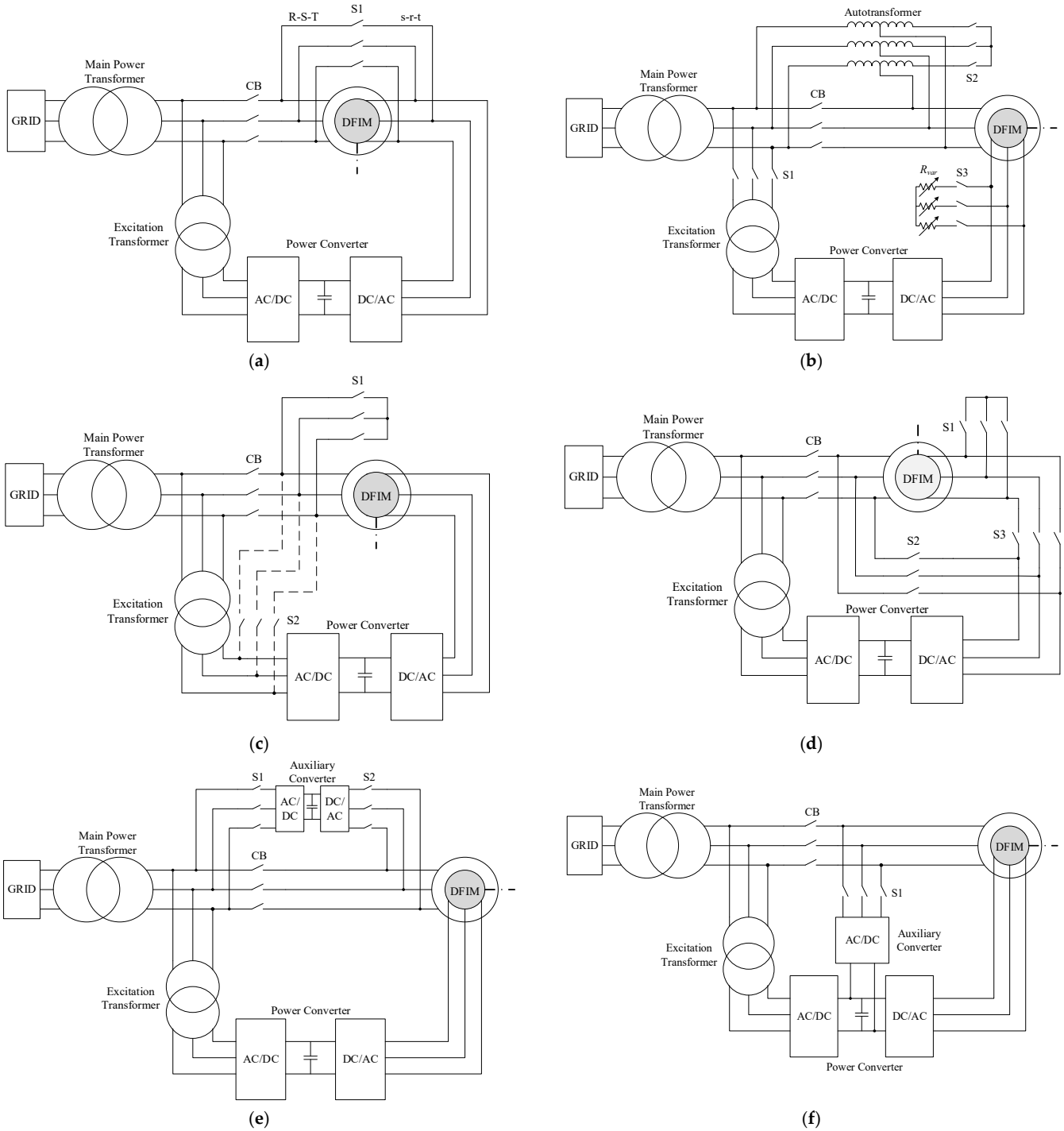

Figure 1. State-of-the-art start-up methods: (**a**) Opposite sequence; (**b**) Autotransformer and variable resistors; (**c**) Stator short-circuit; (**d**) Rotor short-circuit; (**e**) Auxiliary converter on the stator side; (**f**) Auxiliary converter between stator and main converter DC bus.

2.1. Opposite-Phase Sequence-Based Methods

In this approach [12], the stator and rotor are fed in parallel from the converter with opposite-phase sequence, as depicted in Figure 1a. The opposite-phase sequence is achieved by swapping two phases in the connection between stator and rotor. This connection includes an additional switch (S1), which is initially closed. Under these conditions, the machine is brought to the operating speed, S1 is opened, and the machine is connected to the grid by closing the main circuit breaker (CB).

The main advantage of this method is that the starting time is largely shortened in comparison with other methods. However, the technique is characterized by a high torsional stress imposed on the shaft between the opening of S1 and the closing of the CB, associated with the high oscillating electromagnetic torque produced by the machine. As a result, this method is not generally used for start-ups.

2.2. Reduced Voltage-Based Methods

2.2.1. Autotransformer and Variable Resistors in the Rotor

As illustrated in Figure 1b, the method employs an autotransformer (AT) connected to the stator terminals and a variable resistor (R_{var}) inserted in the rotor circuit [13]. The setup requires two additional switches, S2 and S3, which are initially closed to integrate and later disconnect the resistors during the starting process. The variable resistor enables a gradual and controlled start-up. Once the machine reaches approximately 95% of its operating speed, S2 is opened, transitioning the AT to operate as a current-limiting device. Simultaneously, S3 is disconnected, and S1 is closed to supply the rotor with the excitation through the power converter, leading the machine to the full operating speed. Finally, the CB is closed, bypassing the AT and completing the start-up procedure.

This process allows for gradual, smoother start-up compared to other methods. The procedure does not allow for a fast start-up as required in power plants. Furthermore, additional components (autotransformer and rotor resistances) are required to perform the start-up.

2.2.2. Stator Short-Circuit

Other methods utilize the power converter to control the variable speed drive, facilitating a reduced-voltage start-up without requiring the AT and variable resistors as in the previous method. One such approach, commonly used in the industry for large units, involves short-circuiting the stator windings [14–28], as shown in Figure 1c. The stator short-circuit is implemented with an additional switch, S1, which is initially closed. The machine is accelerated up to the required speed by exciting the rotor windings. Once the machine reaches its operating speed, S1 is opened, clearing the short-circuit. The machine rotates freely. When the synchronization conditions are met while exciting the rotor winding, the synchronization with the power system is conducted by closing the CB. The time between the opening of S1 and the closing of the CB should be minimized in order to avoid significant parameter differences that could lead to abrupt synchronizations.

Alternatively [29], as also depicted in Figure 1d, the machine can be accelerated up to half speed by exciting the rotor windings under the stator-short circuit condition, inducing full stator frequency. Then, the short-circuit is cleared by opening S1, and the stator is synchronized to the secondary side of the excitation transformer by closing S2. Subsequently, the converter is controlled to accelerate the machine up to the operating speed. Afterward, S2 is opened, the machine rotates freely, and when the synchronization conditions are met while exciting the rotor winding, the synchronization with the power system is conducted by closing the CB.

Generally, during the start-up, the rotor-side converter (RSC) must deliver a voltage proportional to the rotor frequency, maintaining a constant voltage-to-frequency (V/Hz) ratio and ensuring that the air-gap flux remains stable throughout the start-up process [14–18]. Nevertheless, given that magnetizing and torque currents cannot be managed independently under the constant V/Hz control, vector controls based on stator flux orientation (field-oriented control, FOC) have been proposed to accelerate the machine [19–25], comparatively improving the starting time [26]. Recent additional improvements to the stator-short circuit start-up include injecting a low-voltage DC signal into the stator windings to provide the required reactive power. This eliminates slip losses and cuts down the magnetizing current requirement, reducing the energy consumption [27,28].

This method is characterized by lower power losses during the start-up process compared to other methods. However, the starting torque is limited, and high-power commutation switches capable of withstanding the short-circuit currents are needed as additional components.

2.2.3. Rotor Short-Circuit

Alternatively, the short-circuit can be applied to the rotor windings [14,18,30], as illustrated in Figure 1d. The rotor short-circuit is implemented with an additional switch, S1, which is initially closed, and the excitation power is fed into the stator terminals from the converter through S2, which is also initially closed, all while S3 and the CB are open. This approach allows the machine to operate during start-up similarly to a squirrel-cage induction machine driven by a variable frequency drive. The machine is accelerated up to the operating speed by constant V/Hz control [14] or field-oriented vector control [30]. Once the machine attains the required operating speed, the short-circuit is cleared by opening S1, disconnecting the power converter from the stator by opening S2, and connecting the converter to the rotor by closing S3. The machine rotates freely. Once the synchronization conditions are achieved by exciting the rotor windings, the CB is closed. The stator is directly connected to the grid, while the converter assumes control of the rotor.

This method enables faster, and more energy-efficient start-ups compared to other methods, particularly the stator short-circuit method. However, the power converter must be able to bring the machine up to the operating speed by feeding the stator, which can increase the required converter voltage power rating. Moreover, additional high-power commutation switches are required to withstand the rotor short-circuit currents.

2.3. Auxiliary Converted-Based Methods

In the method detailed in [29], an auxiliary power converter is connected to the stator terminals to perform the start-up of the DFIM, as illustrated in Figure 1e. Initially, switches S1 and S2 are closed, enabling the auxiliary converter to supply the stator with full-frequency power while simultaneously exciting the rotor to achieve the required speed. Once the machine reaches the operating speed, synchronization with the power system is achieved by closing the CB, thereby bypassing the auxiliary converter. Finally, switches S1 and S2 are opened, completing the starting sequence.

An alternative approach was reported in [31], depicted in Figure 1f, which involves an auxiliary voltage source converter (VSC) and an additional switch, S1, to supply the stator from the main converter DC bus, which is initially closed. The vector control for the VSC and the RSC are combined, ensuring a smooth acceleration process. Once the machine reaches the operating speed, S1 is opened, the machine rotates freely, and while the rotor windings are being excited, the machine is synchronized to the power system by closing the CB.

Auxiliary converter-based methods provide smoother start-up compared to the earlier techniques but necessitate additional electronic components and switches, which considerably increases the system's complexity and cost.

2.4. Previous Standstill Synchronization-Based Method

Previously, in [32], the authors presented a soft-starting method for DFIMs based on the synchronization of the machine with the power system at standstill conditions. The configuration of the proposed system is illustrated in Figure 2. The synchronization was proposed on the stator side, via the closing of the main CB.

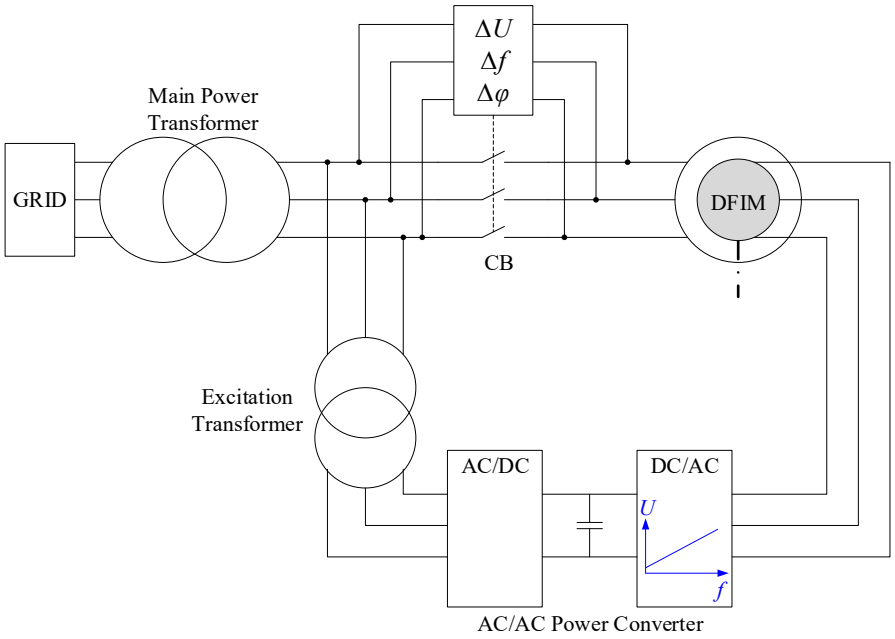

Figure 2. Previous soft-starting method based on standstill synchronization on the stator side.

At the initial conditions, the machine is at standstill conditions and the main CB is initially open. The RSC ensures that the electromotive force (EMF) induced on the stator windings matches the magnitude and frequency conditions required on the stator side of the CB before synchronization. Once these conditions are met, the CB is closed. Then, the RSC gradually reduces its output frequency, causing the rotor to accelerate. The RSC control during the acceleration process is proposed under the constant flux strategy.

The main benefits of this method over state-of-the-art methods are that no other components than the CB are required. Complex switchgear maneuvers are avoided throughout the starting procedures. The method is simple, secure, and cost-effective.

However, several drawbacks of this method have been identified. The main disadvantage is that the magnetizing current is fully provided by the rotor circuit. As a consequence, the rotor power converter must be able to supply the full magnetizing current until the start of the acceleration process. This requires larger sizing requirements for the power converter. Moreover, the high-frequency pulses generated by the RSC, due to pulse-width modulation (PWM), are induced in the stator winding before grid synchronization, resulting in increased stress on the insulation. The motivation of the present work is to effectively address these limitations.

In summary, the advantages and limitations of each state-of-the-art method for DFIM starting are provided in Table 1.

Table 1. DFIM starting methods: state of the art sum-up.

Type	Method	References	Advantages	Limitations
Opposite-phase sequence-based		[12]	✓ Fast starting	× High oscillation torque and torsional forces on the shaft
Reduced voltage-based	With autotransformer	[13]	✓ Supports partial winding starting ✓ Smoothness	× Slow starting × Additional autotransformer and rotor resistances required
	Stator short-circuited	[14–29]	✓ Low power losses ✓ Acceptable soft starting	× High power commutation switch required to support the stator short-circuit currents × Reduced starting torque
	Rotor short-circuited	[14,18,30]	✓ Fast starting	× Increased converter power rating required to carry the machine up to its rated speed by feeding the stator × High-power commutation switch required to support the rotor short-circuit currents
Auxiliary converter-based		[29,31]	✓ Soft-starting ✓ Auxiliary converters can be used for power enhancement in case of low load ✓ Simple synchronization	× Additional power electronic devices and switches required
Standstill synchronization-based	Stator-side synchronization	[32]	✓ Simple execution ✓ No additional devices needed ✓ Soft starting with no torque pulses and low inrush currents	× Increased converter power rating (design), or increased electrical stress on the converter (operation) in order to supply the magnetizing current × Electrical stress from PWM pulses affecting the stator winding before synchronization × Slow starting as a consequence of the soft-starting process
	Rotor-side synchronization (proposed method)		✓ Simple execution ✓ No additional devices needed ✓ Soft starting with no torque pulses and low inrush currents ✓ Low converter power rating (design), or low electrical stress on the converter (operation), as the magnetizing current is provided from the stator fed from the grid ✓ Reduced electrical stress on the stator windings before synchronization	× Slow starting as a consequence of the soft-starting process × Additional switch required on the rotor side × The voltage during the initial moments of the starting process must be higher than that of a converter operating in steady-state conditions with small slip values.

3. Operating Principles of the Proposed Starting Method

3.1. General Method Outline

The simplified electrical configuration of the system to start-up the DFIM is shown in Figure 3. The stator of the DFIM is connected to the power system through a main step-up power transformer and the main CB, while the rotor windings are connected through back-to-back power converters (RSC and GSC). The rotor-side connection is equipped with an additional switch (S1), which is provided with an automatic synchronizing relay. The rotor is mechanically coupled to the hydro turbine.

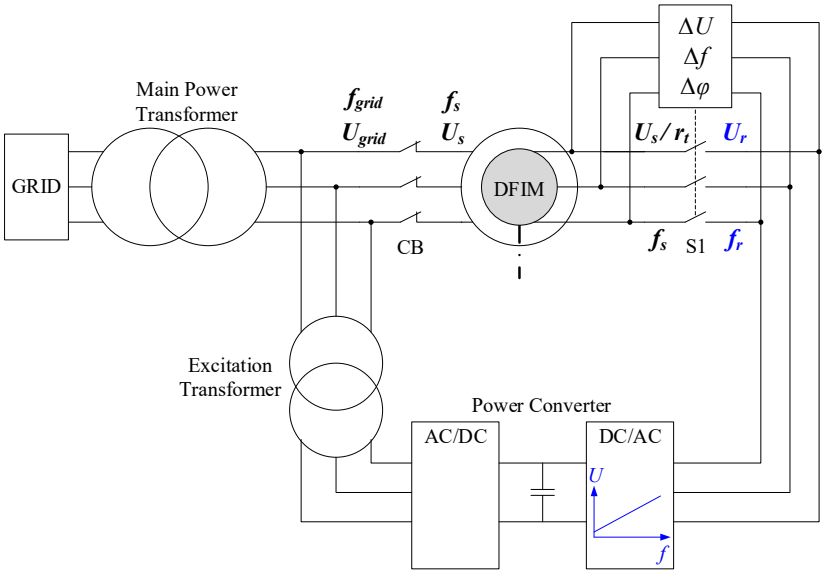

Figure 3. Electrical scheme for the proposed starting method (U_{grid}: power system voltage; U_s: stator voltage; U_r: converter-fed rotor voltage; f_{grid}: power system frequency; f_s: stator currents frequency; f_r: converter-fed rotor currents frequency; r_t: stator-to-rotor transformation ratio; ΔU: voltage magnitude difference; Δf: frequency difference; $\Delta\varphi$: phase difference). Manageable variables presented in blue.

The proposed method is based on the synchronization of the DFIM to the power system under standstill conditions on the rotor side. To this end, the machine is initially fed through the stator windings directly from the power system, i.e., the CB is initially closed. The rotor windings are initially open, i.e., S1 is initially open, implying that the rotor will be found at standstill conditions unless an external torque is applied to the shaft. The converter is controlled to ensure that the rotor-side synchronization conditions are met. Once the synchronization conditions are met and S1 is closed, the power converter performs variable voltage and frequency control to accelerate the machine from standstill to the rated speed.

The main advantage of the proposed method lies in the reduction in the complexity and costs compared to state-of-the-art methods. No additional switchgear (breakers, autotransformers, resistors, auxiliary converters), other than the main CB and the switch are required for soft-starting of the DFIM. Moreover, if IGBT switching control in the RSC is leveraged with conventional grid synchronization methods, such as phase-locked loops (PLL), the additional switch can be avoided.

Furthermore, the method enhances security in the operation of DFIMs, as the need for short-circuits is eliminated. Inrush currents and potential voltage sags during the starting process are avoided, which signifies notable benefits for power system stability, especially for weaker systems.

3.2. Detailed Method Description

Initially, the machine is found in standstill conditions, including the case of transition from generating to pumping mode. In these conditions, the rotor mechanical speed is zero ($\omega_m = 0$), and the main CB is in the closed state, i.e., the stator is connected to the power system; therefore, $U_s = U_{grid}$ and $f_s = f_{grid}$. The initial status of S1 is open. The voltage on the converter side of S1 corresponds to U_r, while the actual rotor voltage, on the machine side of S1, is imposed by the voltage ratio as U_s/r_t. Based on this initial scenario, the control of the power converter is conducted in order to achieve the rotor-side synchronization conditions. The flowchart of the proposed starting method is presented in Figure 4.

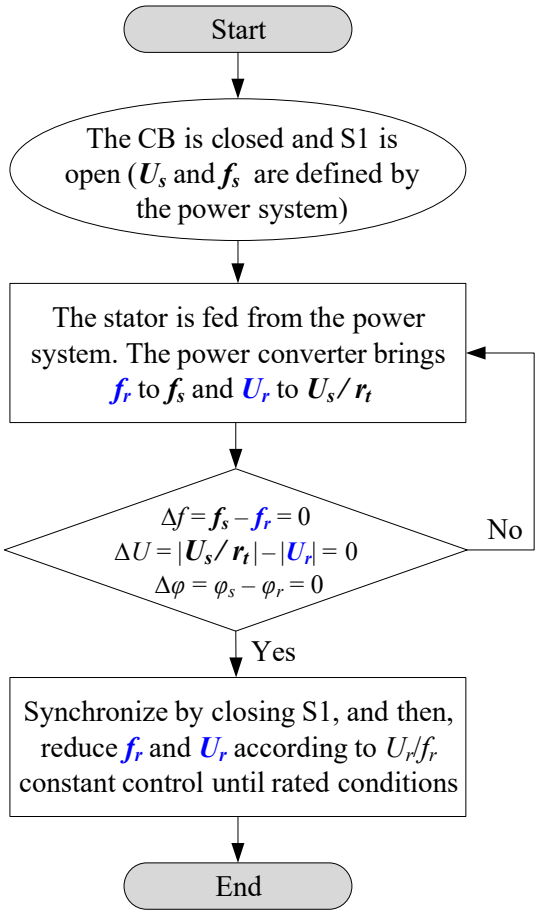

Figure 4. Flowchart of the proposed starting method. Manageable variables presented in blue.

To achieve the rotor-side synchronization conditions, the power converter must control its terminal voltage magnitude U_r and frequency f_r. The frequency of the rotor currents, for a DFIM with p pole pairs, should be set using Equation (1):

$$\omega_m = \frac{2 \cdot \pi}{p} \cdot (f_s - f_r) \quad (1)$$

From Equation (1), with initial standstill conditions ($\omega_m = 0$), and the stator windings fed from the power system ($f_s = f_{grid}$), it is derived that the converter's frequency (f_r) should be driven to the grid frequency ($f_r = f_s = f_{grid}$). This allows to satisfy the first synchronization condition ($\Delta f = 0$), as shown in Figure 4.

Furthermore, the converter's output voltage (U_r) should be driven to the equivalent rotor voltage ($U_r = U_s/r_t = U_{grid}/r_t$), with r_t being the stator/rotor voltage ratio. This condition ensures that the induced EMF in the rotor windings matches the rotor voltage at the synchronization instant, allowing to satisfy the second synchronization condition

($\Delta U = 0$), as per Figure 4. Failing to achieve this condition would lead to an unnecessary reactive power flow, disrupting the transient smoothness of the proposed method. The constant flux or V/Hz control is proposed in this process.

It shall be noted that if the shaft is initially rotating ($\omega_m \neq 0$), as occurs for starting in the turbine mode, the converter should impose a rotor frequency f_r that corresponds to the difference between the mechanical rotation frequency and the stator frequency, following Equation (1). However, the developments are carried out assuming starting in the pumping mode, as the counter torque present in this mode of operation makes it more critical.

Once the converter has matched the rotor voltage U_r and frequency f_r to the mentioned values, the voltage magnitude difference condition ($\Delta U = |U_s/r_t| - |U_r| = 0$) and the frequency difference condition ($\Delta f = f_s - f_r = 0$) are met. Provided that the phase sequence is the same on both sides of the CB, the CB is closed when the third synchronization condition is met: when the phase shift between voltage phasors is zero ($\Delta\varphi = 0$). The machine, previously fed from the stator, has been synchronized to the power system on the rotor side, at standstill conditions. Then, given that the rotor's frequency is equal to the stator's ($f_s = f_r$), fluxes match. Therefore, no EMFs or torque are produced. Consequently, the shaft remains at standstill conditions ($\omega_m = 0$) after synchronization.

After synchronization, the actual rotor voltage (U_r) and frequency (f_r) are imposed by the power converter. The converter smoothly reduces the output frequency f_r, causing the shaft to rotate according to Equation (1). In this process, a constant flux or V/Hz control is also proposed; thus, the rotor voltage (U_r) should be reduced proportionally to the rotor frequency (f_r). This process is conducted until the rotor frequency matches the rated value, and therefore the machine attains the rated speed. Throughout this process, the machine accelerates from standstill up to the rated speed, ramping down from a unitary slip ($s = 1$) to the rated slip. The softness of this process is directly related to the rate of change of frequency applied by the converter.

3.3. Theoretical Considerations

3.3.1. General Description of the DFIM

The DFIM can be described with voltage equations, flux linkage equations, and mechanical equations [33], under the assumption of sinusoidal field distribution along the airgap periphery and phase balance; thus, no zero-sequence currents, and constant magnetic saturation during the process. The equations addressed in this section, in the per-unit (p.u.) system, completely define the transient behavior of the DFIM's state variables.

First, the general phasor equations for the stator and rotor voltages in a DFIM can be written in the stator-flux reference frame as per Equations (2) and (3), respectively:

$$\underline{U_s} = \frac{d\underline{\Psi_s}}{dt} + j\omega_0\underline{\Psi_s} + R_s\underline{I_s} \tag{2}$$

$$\underline{U_r} = \frac{d\underline{\Psi_r}}{dt} + j(\omega_0 - \omega_{mec})\underline{\Psi_r} + R_r\underline{I_r} \tag{3}$$

where Ψ_s is the stator flux, Ψ_r is the rotor flux, ω_0 is the angular speed, R_s is the stator resistance, R_r is the rotor resistance, and I_s and I_r are the stator and rotor currents, respectively.

Secondly, the general expressions for the stator and rotor flux linkages in a DFIM can be written, in the same reference frame, as per Equations (4) and (5), respectively:

$$\omega_0\underline{\Psi_s} = X_s\underline{I_s} + X_m(\underline{I_s} + \underline{I_r}) \tag{4}$$

$$\omega_0\underline{\Psi_r} = X_r\underline{I_r} + X_m(\underline{I_s} + \underline{I_r}) \tag{5}$$

where X_s is the stator leakage reactance, X_m is the magnetizing reactance, and X_r is the rotor leakage reactance of the DFIM.

By introducing Equations (4) and (5) into Equations (2) and (3), the following Equations (6) and (7) are derived:

$$\underline{U}_s = [R_s + j(X_s + X_m)]\underline{I}_s + \frac{(X_s + X_m)}{\omega_0}\frac{d\underline{I}_s}{dt} + \left(\frac{d}{dt} + j\omega_0\right)\frac{X_m}{\omega_0}\underline{I}_r \tag{6}$$

$$\underline{U}_r = [R_r + js(X_r + X_m)]\underline{I}_r + \frac{(X_r + X_m)}{\omega_0}\frac{d\underline{I}_r}{dt} + \left(\frac{d}{dt} + js\omega_0\right)\frac{X_m}{\omega_0}\underline{I}_s \tag{7}$$

Finally, the mechanical equations, including the motion equation and the expression of the mechanical torque, are provided in Equations (8) and (9), respectively:

$$\frac{d\omega_{mec}}{dt} = \frac{T_m - T_r}{2H} \tag{8}$$

$$T_m = X_m \cdot Im\{\underline{I}_s \cdot \underline{I}_r^*\} \tag{9}$$

where T_m is the mechanical torque, T_r is the mechanical counter-torque applied to the rotor, and H is the rotor inertia constant.

3.3.2. Rotor-Side Synchronization Analysis

In the proposed method, the grid provides the magnetizing current and imposes the rotor-side synchronization voltage. The magnetization takes place following a flux creation transient. According to Equation (6), and assuming that the rotor is open-circuited, Equation (10) expresses the evolution of the stator current:

$$\underline{I}_s = \frac{\underline{U}_s}{R_s + j(X_s + X_m)} \cdot \left[1 - e^{-\left(\frac{R_s}{X_s + X_m} + j\right)\cdot\omega_0 \cdot t}\right] \tag{10}$$

Given the typical values of the motor parameters, the maximum value of the stator current is below 1 p.u. Once the magnetization transient finishes, synchronization is possible. In order to achieve this as smoothly as possible, the rotor current should ideally be zero ($I_r \approx 0$) at the synchronization instant. The particularization of Equations (6) and (7) for $I_r \approx 0$, $f_s = f_r$ and the null time derivatives yields Equations (11) and (12):

$$\underline{I}_s|_{sync} = \frac{\underline{U}_s}{R_s + j(X_s + X_m)} \tag{11}$$

$$\underline{U}_r|_{sync} = \frac{jX_m}{R_s + j(X_s + X_m)}\underline{U}_s \tag{12}$$

As derived from Equations (11) and (12), the magnetizing current is fully drawn from the grid. Given that for an infinitely rigid power system U_s is constant at its rated value ($U_s = U_{grid} = 1$ p.u.), and that the grid voltage is taken as phase reference ($\varphi_s = \varphi_{grid} = 0$), Equation (11) turns into Equation (13):

$$1 = [R_s + j(X_s + X_m)] \cdot I_s|_{sync} \tag{13}$$

Consequently, the magnitude of the current drawn from the grid I_s at the synchronization instant is given by Equation (14), while the rotor voltage magnitude (U_r) which should be provided by the converter on the converter side of the switch before synchronization is given by Equation (15):

$$I_s|_{sync} = \frac{1}{\sqrt{R_s^2 + (X_s + X_m)^2}} \tag{14}$$

$$U_r = \frac{X_m}{\sqrt{R_s^2 + (X_s + X_m)^2}} \tag{15}$$

Therefore, the rotor voltage will be lower than its rated value as the denominator of Equation (15) is larger than its numerator. The synchronization can be conducted without a transient at the switching of the rotor-side switch.

3.3.3. Acceleration Analysis

Once the DFIM has been synchronized to the power system, the rotor is accelerated. In this process, the magnetizing current provided by the grid is gradually reduced as the converter assumes part of this current.

To analyze the acceleration process, the starting electromagnetic transients will be neglected because the starting is assumed to be smooth, i.e., the electrical parameters will change slowly, and their time decay is fast. Thereby, the time derivatives in Equations (6) and (7) will be considered zero. In addition, under a constant flux or V/Hz strategy, the ratio between U_r and f_r will remain constant throughout the process (U_f/f_r = constant = 1 p.u.). Under these considerations, $\underline{I}_r$ and $\underline{I}_s$ can be calculated according to Equations (16) and (17), respectively:

$$\underline{I}_r = \frac{\underline{U}_r[R_s + j(X_s + X_m)] - jsX_m\underline{U}_s}{sX_m^2 + [R_r + js(X_r + X_m)][R_s + j(X_s + X_m)]} \tag{16}$$

$$\underline{I}_s = \frac{\underline{U}_s - jX_m\underline{I}_r}{R_s + j(X_s + X_m)} \tag{17}$$

Equations (16) and (17), along with the mechanical characteristics expressed in Equations (8) and (9) characterize the DFIM's starting dynamics. The acceleration process ends when the rated rotor frequency is achieved, i.e., the machine slip is ramped down from unity to the rated slip. This progression should be smooth, as if this ramp is too steep, there is a risk of overcurrent associated to the DFIM's inertia.

4. Computer Simulations

Extensive computer simulations were performed using the Matlab-Simulink® (version R2024a) environment, with the objective of verifying the proposed DFIM soft-starting method. For these simulations, a model comprising a 0.52 kW DFIM is employed. In this section, this model and the results obtained from the simulations are presented.

4.1. Simulation Model

The simulation model is based on a 0.52 kW DFIM, connected to a 400 V, 50 Hz, three-phase infinite bus through the main CB. This CB is initially closed, feeding the machine from the stator side, directly from the power system.

On the grid side of the rotor circuit, the power converter is fed from a 120 V three-phase system, representing the secondary side of the excitation transformer. The GSC is controlled to sustain the voltage at the DC stage (V_{dc}), which is equipped with a C = 1600 μF capacitor. The setpoint for V_{dc} depends on the rotor frequency f_r. It should be noted that the capacitor is sized to stabilize the DC bus voltage and ensure converter functionality. As long as C is appropriately sized, it does not influence the performance of the proposed starting method.

On the machine side of the converter, the RSC generates the required PWM signals to ensure the necessary rotor voltage U_r and frequency f_r at each time. A switch S1 is located between the RSC and the rotor winding, which is initially open. This switch is provided with an automatic synchronizer. Once the RSC provides the required voltage magnitude and frequency (this frequency is set at f_r = 49.95 Hz to ensure seamless synchronization),

S1 is closed to synchronize the DFIM to the power system through the rotor circuit. After synchronization, f_r is smoothly ramped down to 2 Hz, accelerating the rotor. The total acceleration time is set at t = 5 s to achieve soft starting.

Figure 5 shows the simulation model, while Table 2 lists the rated values of the DFIM's main rated parameters.

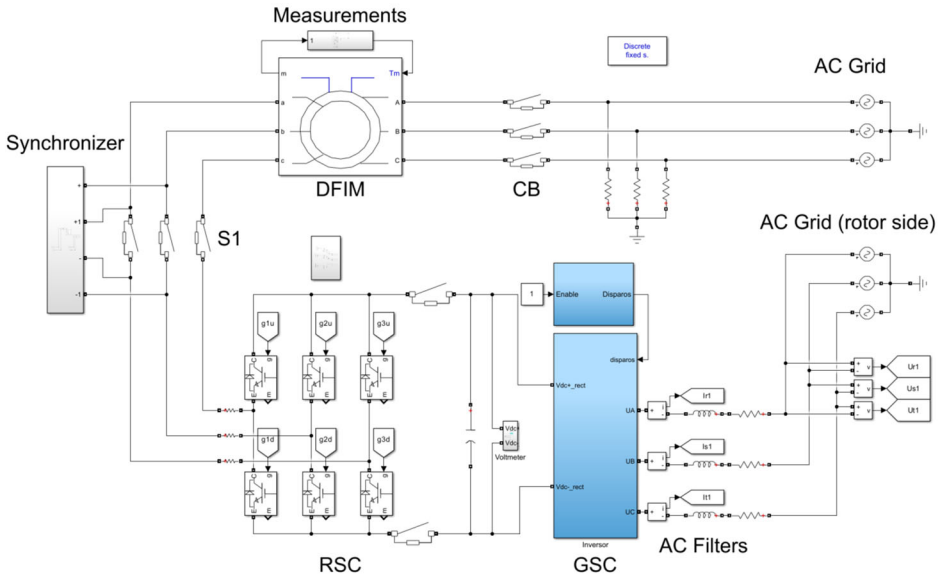

Figure 5. Simulation model.

Table 2. Simulated DFIM's main rated parameters.

Parameter	Magnitude	Units
Real power (P)	0.52	kW
Stator voltage (U_s)	400	V
Frequency (f_s)	50	Hz
Stator/rotor voltage ratio (r_t)	10/1	V/V
Stator resistance (R_s)	30.0	Ω
Stator inductance (L_s)	0.120	H
Equivalent rotor resistance (R_r')	30.0	Ω
Equivalent rotor inductance (L_r')	0.120	H
Mutual inductance (L_m)	2.432	H
Moment of inertia (J)	0.0015	kg·m^2
Number of pole pairs (p)	2	
Speed (n)	1400	rpm

4.2. Simulation Results

Figure 6 shows the evolution of the main machine variables involved during the starting process (ω_m, T_m, I_r, I_s, and U_r). These variables are expressed in the per-unit (p.u.) system based on the DFIM's rated values.

As can be observed in Figure 6, before S1 is closed, the initial magnetizing current is provided by the grid-fed stator, with a value of approximately $I_s \approx 0.50$ p.u. The rotor winding is initially open-circuited; thus, no current flows through this circuit, $I_r \approx 0$. The machine is, therefore, found under standstill conditions ($\omega_m = 0$). Furthermore, before synchronization, the converter imposes the required rated rotor voltage on its side of S1 (U_r = 0.76 p.u. in this case). The rotor frequency imposed by the converter on its side of S1 was set at f_r = 49.95 Hz, close to the grid frequency.

The synchronization is conducted, under standstill conditions, at t = 0.34 s, and at this time, the acceleration process starts and lasts for approximately 4 s. The initial flux creation transient occurs after synchronization, with a stator current increase up to $I_s \approx 0.55$ p.u. No rotor current peaks are observed following synchronization, as the synchronizer enables the

closing of S1 only when the voltage magnitude, frequency, and phase shift conditions are achieved. However, transient oscillatory currents flow through the rotor circuit during the initial stages of the acceleration process, attaining an overshoot slightly above $I_r \approx 0.60$ p.u., as a result of the mechanical characteristics of the DFIM. This transient imposes a light oscillatory effect on the torque during the initial stage of the acceleration process. After these transients, the rotor current and torque achieve smoother conditions at approximately $t = 1$ s.

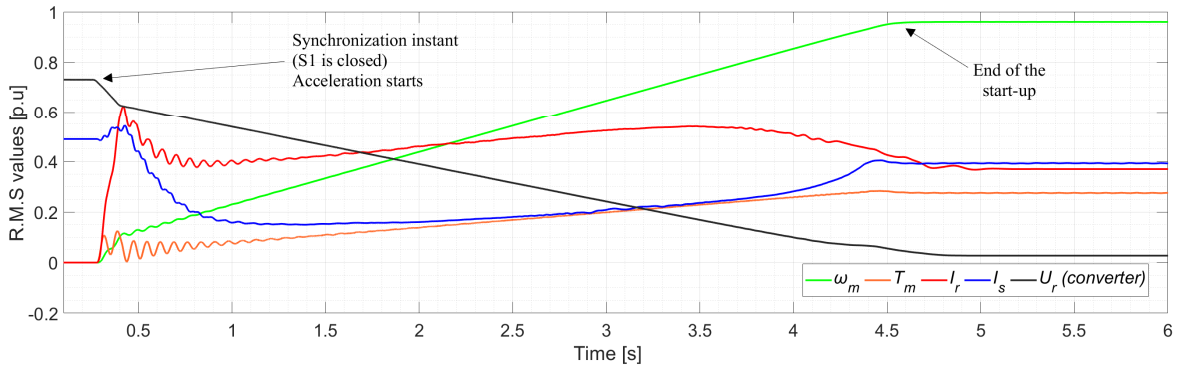

Figure 6. Simulation results for the proposed soft starting [mechanical rotor speed (ω_m); torque (T_m); RMS values of rotor and stator currents (I_r and I_s, respectively); rotor voltage (U_r)].

The acceleration initiates when the converter control leaves the constant rotor voltage setpoint. The rotor voltage imposed by the converter is ramped down smoothly from $U_r = 0.76$ p.u. to its rated value of $U_r = 0.05$ p.u. under the V/Hz control strategy, i.e., from $f_r = 49.95$ Hz to $f_r = 2.5$ Hz, during approximately 4 s. As a consequence, the rotor initiates its rotational motion ($\omega_m > 0$) and accelerates ($d\omega_m/dt > 0$) up to the operating speed based on the setting of f_r ($\omega_m = 0.95$ p.u., i.e., final slip of $s = 0.05$). Throughout this process, the magnetizing current is supplied by the stator and rotor circuits according to the behavior of the machine's characteristic impedances. At the end of the acceleration process, the magnetizing current is partly drawn from each side: $I_r \approx 0.35$ p.u. and $I_s \approx 0.40$ p.u.

Finally, in Figure 7, the converter-side and machine-side rotor voltages are shown, i.e., the voltages on both sides of S1. Before S1 is closed, the converter-side voltage pulses in accordance with the PWM from the RSC, while the machine-side voltage is purely sinusoidal, as it corresponds to the EMF induced on the rotor windings when feeding the stator from the grid. After closing S1, the pulsed signal injection by the RSC to the rotor windings is observed.

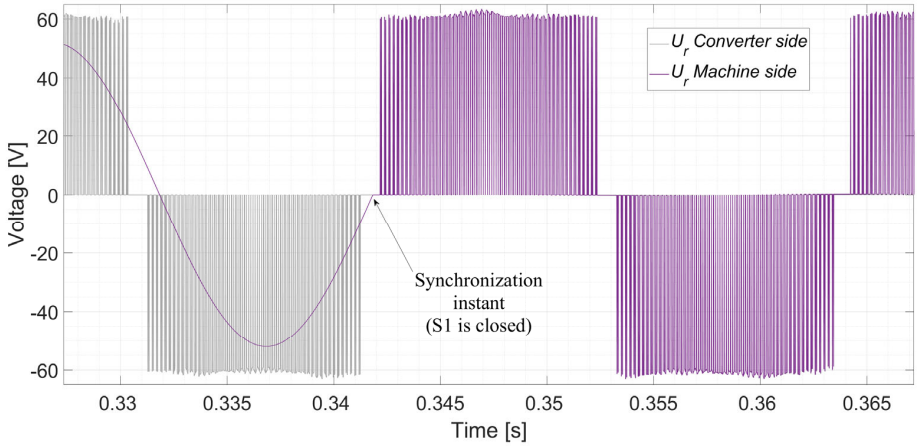

Figure 7. Simulation results for the proposed soft-starting method [Rotor voltage (U_r) on the converter and machine sides].

5. Experimental Tests

5.1. Experimental Setup

The experimental setup can be observed in Figure 8 in the form of an electrical simplified scheme. The overview of the setup can be seen in Figure 9. The numbering in Figures 8 and 9 is consistent. The setup comprises a 7.5 kW wound-rotor induction machine (1) (160M4, Leroy Somer, Angouleme, France) with a 7.5 kW power converter (Vacon NXP, Danfoss Drives, Nordborg, Denmark) connected to the rotor (2) via brushes and slip rings. This power converter hosts both the RSC and the GSC. The DFIM's main parameters are listed in Table 3.

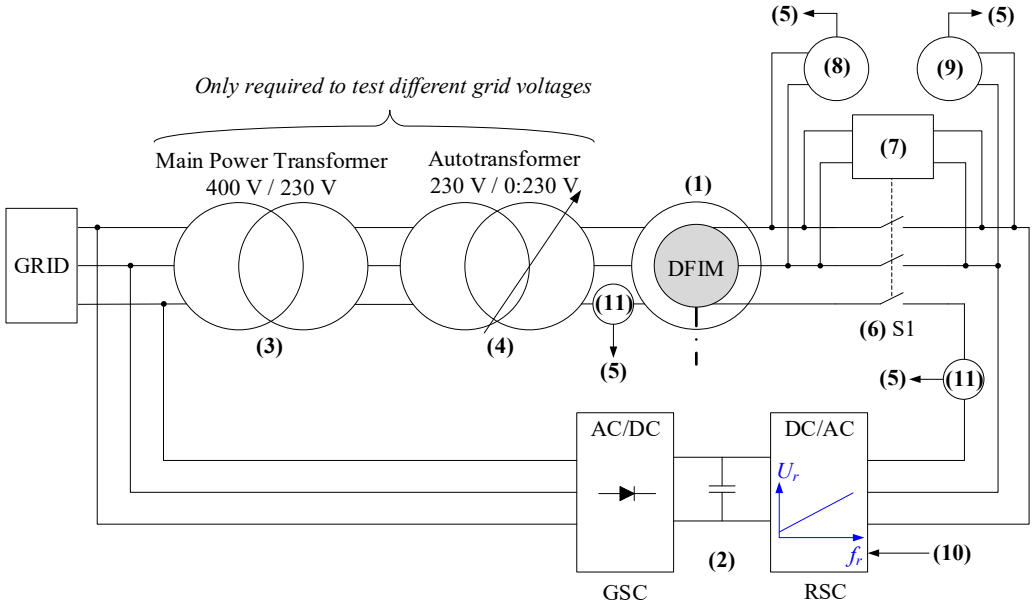

Figure 8. Experimental setup: electrical scheme [(1): DFIM; (2): Power converter; (3): Main power transformer; (4): Autotransformer; (5): Oscilloscope; (6): CB; (7): Synchronizer; (8): Rotor-side voltmeter; (9): RSC-side voltmeter; (10): Computer interface; (11): Ammeters].

Figure 9. Experimental setup: overview [(1): DFIM; (2): Power converter; (3): Main power transformer; (4): Autotransformer; (5): Oscilloscope; (6): CB; (7): Synchronizer; (8): Rotor-side voltmeter; (9): RSC-side voltmeter; (10): Computer interface; (11): Ammeters].

Table 3. Tested DFIM's main parameters.

Parameter	Magnitude	Units
Real power (P)	7.5	kW
Stator voltage (U_s)	230/400	V
Stator current (I_s)	32/18	A
Rotor voltage (U_r)	190	V
Rotor current (I_r)	24	A
Power factor (PF)	0.70	
Frequency (f_s)	50	Hz
Stator/rotor voltage ratio (r_t)	2.10/1	V/V
Stator resistance (R_s)	0.25	Ω
Stator inductance (L_s)	0.875	mH
Equivalent rotor resistance (R_r')	1.55	Ω
Equivalent rotor inductance (L_r')	5.425	mH
Mutual inductance (L_m)	0.135	H
Moment of inertia (J)	0.0439	kg·m^2
Number of pole pairs (p)	2	
Rated speed (n)	1447	rpm
Mounting code	B3	
Weight	136	kg
Diameter/height ratio	6	
Ingress protection (IP) code	55	
Impact protection (IK) rating	08	
Insulation class	F	
Duty type	S3 (100%)	
Maximum ambient temperature	40	°C
Bearings (driving end)	6309 Z C3	
Bearings (non-driving end)	6309 C3	Ω

On the stator side, the machine is directly fed from the AC grid (U_{grid} = 400 V, f_{grid} = 50 Hz) through the 400/230 V main power transformer (3), and additionally, a 230/0:230 V variable autotransformer, i.e., variac (4), in order to test the proposed starting methods at different voltage levels. However, this autotransformer is not required to conduct tests under conventional conditions, as the DFIM is commonly fed by providing the rated voltage to the stator. A current probe connected to a 4-channel digital oscilloscope (5) (PZ4000 Power Analyzer, Yokogawa Electric Corporation, Tokyo, Japan) is used to monitor the stator current. Additionally, several network analyzers (11) are utilized to monitor the stator- and rotor-side measurements during the start-up process.

On the rotor side, switch S1 is equipped with a synchronizer (7). The rotor voltage is measured on the machine (8) and converter (9) sides of S1. Differential probes are also installed on both sides of S1, to register the values via the 4-channel digital oscilloscope (5). In addition, another current probe, also connected to (6), is employed to monitor the rotor current. The power converter (2) is directly fed from the AC grid. This converter comprises a 6-pulse bridge rectifier (GSC) to sustain the voltage at the DC bus, which is rated at V_{dc} = 540 V, and a controlled 6-pulse IGBT inverter (RSC), allowing for constant V/Hz control. The rotor converter is controlled through a computer interface (10). The rotor voltage is initially set at U_r = 190 V with a frequency of $f_r = f_{grid}$ = 50 Hz. During the start-up process, they are progressively reduced to U_r = 20 V and f_r = 5 Hz, respectively, which are the values at the end of the acceleration process.

5.2. Experimental Results

The results of the experimental implementation of the proposed soft-starting method are presented in Figure 10. This figure depicts the evolution of the main machine variables involved during the starting process (ω_m, T_m, I_r, I_s, and U_r). These variables are expressed in the per-unit (p.u.) system based on the DFIM's rated values.

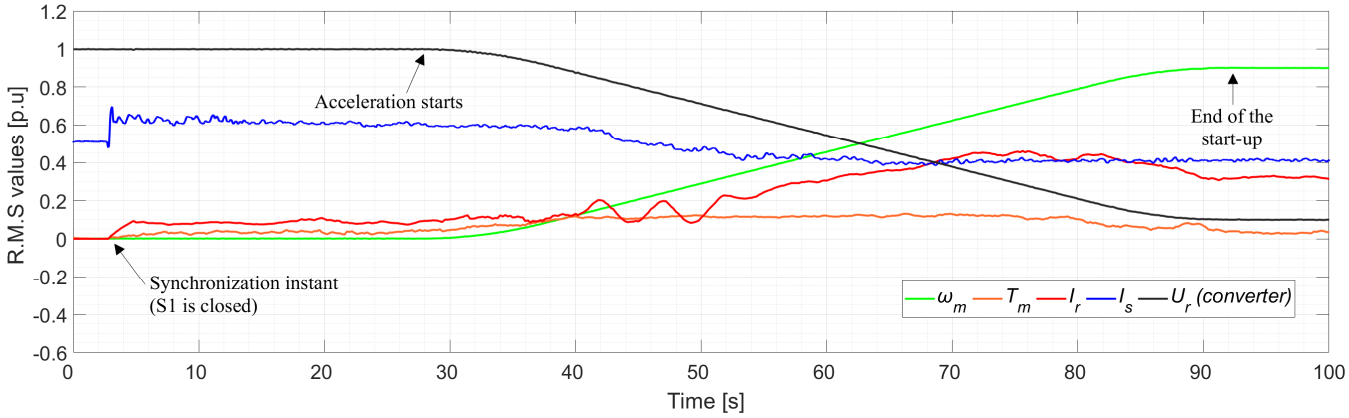

Figure 10. Experimental results for the proposed soft starting [mechanical rotor speed (ω_m); torque (T_m); RMS values of rotor and stator currents (I_r and I_s, respectively); rotor voltage (U_r)].

In Figure 10, before S1 is closed, the initial magnetizing current is provided by the grid-fed stator, with a value of approximately $I_s \approx 0.50$ p.u. The rotor winding is initially open-circuited; thus, no current flows through this circuit, $I_r \approx 0$. The machine is, therefore, found under standstill conditions ($\omega_m = 0$). Furthermore, during this initial stage, the converter imposes the rated rotor voltage on its side of S1 ($U_r = 1$ p.u.). The rotor frequency imposed by the converter on its side of S1 was set at $f_r = 49.95$ Hz, close to the grid frequency.

The synchronization is performed, under standstill conditions, at $t = 2.825$ s. At this time, the initial flux creation transient occurs, with a stator current increase up to $I_s \approx 0.70$ p.u., followed by a stabilization around $I_s \approx 0.60$ p.u., which corresponds to the magnetizing current required by the machine to continue being constantly supplied by the stator. Following the synchronization, given that the voltage magnitude, frequency, and phase shift conditions are accurately achieved at synchronization, the rotor current deviates very slightly from its zero theoretical value, due to ordinary transients related to slight parameter shifts. This current does not surpass 0.15 p.u. ($I_r < 0.15$ p.u.). Following the rotor current behavior, the mechanical torque applied by the machine on the rotor is also very low throughout this stage ($T_m < 0.05$ p.u.). The converter control is set to sustain the rotor voltage constant at the rated value ($U_r = 1$ p.u.). As after synchronization $f_r = f_s$, the machine remains at standstill conditions ($\omega_m = 0$).

The acceleration initiates at $t = 28.50$ s, as at this time the converter control leaves the constant rotor voltage setpoint. The rotor voltage imposed by the converter is ramped down smoothly from $U_r = 1$ p.u. (190 V) to its rated value of $U_r = 0.1$ p.u. (20 V) under the V/Hz control strategy, i.e., from $f_r = 49.95$ Hz to $f_r = 5$ Hz, during approximately 60 s. As a consequence, the rotor initiates its rotational motion ($\omega_m > 0$) and accelerates ($d\omega_m/dt > 0$), up to the operating speed based on the setting of f_r ($\omega_m = 0.90$ p.u., i.e., final slip of $s = 0.10$). Gradually, the current drawn by the stator from the grid I_s decreases, while the rotor current I_r increases. The rotor side provides the accelerating current, as well as progressively an increasing part of the magnetizing current to the detriment of the stator side. After the acceleration process ends, the magnetizing current is partly drawn from each side: $I_r \approx 0.30$ p.u. and $I_s \approx 0.40$ p.u.

Therefore, throughout the whole starting process, the experimental results are consistent with the results obtained from the computer simulations. However, the process observed in the experimental approach is smoother than the one in the computer simulations, as the current and torque transients observed in Figure 6 are not present in Figure 10. This evidences that the transients in the computer simulations did not respond to actual physical phenomena but to simulation issues.

Finally, in Figure 11, the waveforms of both the machine-side and converter-side rotor voltages are provided. Also, similarly to the simulations, during the pre-synchronization stage the machine-side voltage responds to the EMF induced on the rotor windings as a result of the stator-side feeding from the grid. The converter-side voltage is pulsed due to the PWM feeding. After closing S1, the power converter injects the pulsed voltage signal to the rotor windings.

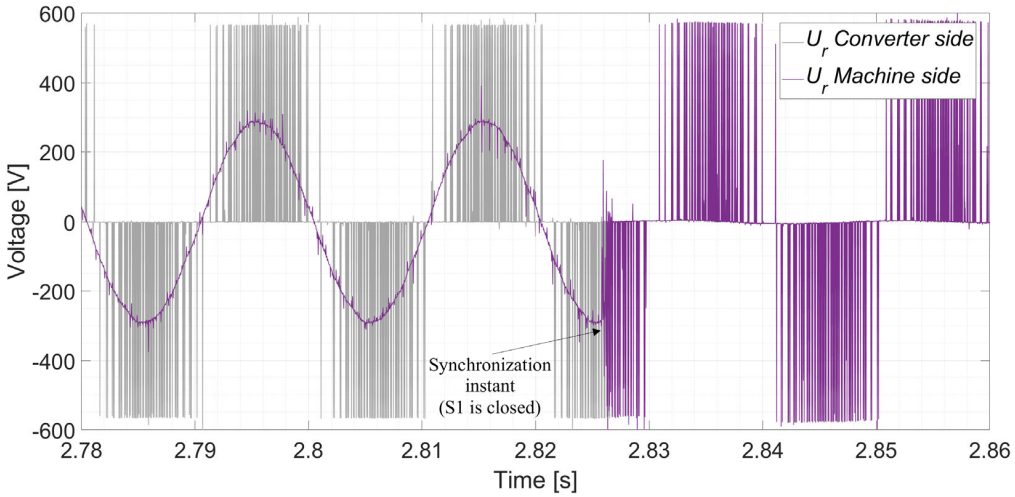

Figure 11. Experimental results for the proposed soft-starting method [Rotor voltage (U_r) on the converter and machine sides].

6. Discussion

6.1. Findings

An improved DFIM starting method has been proposed and verified through both computer simulations and experimental tests, under free shaft conditions, which is typical in hydro pumped-storage units in the pumping mode. The proposed technique is significantly simpler and more cost-effective than alternative methods aimed at achieving the same objective, as it eliminates the need for complex maneuvers and additional equipment as in mainstream state-of-the-art methods.

Beyond the aforementioned simplicity and cost-effectiveness, the findings derived from the results presented in this work are related to the reduction in inrush currents, benefiting both the DFIM and the grid stability. Experimental tests indicate that the proposed method requires approximately $I_s \approx 0.6$ p.u. stator current to provide the magnetizing current during the initial stage. By the end of the acceleration process, the current required from the RSC is only around $I_r \approx 0.4$ p.u., which accounts for a portion of the magnetizing current as well as the accelerating current. Meanwhile:

- opposite phase sequence-based techniques reach up to 6 p.u. [12];
- reduced voltage-based techniques using autotransformers and variable resistors can reduce the inrush current down to 0.8 p.u. [13];
- stator short-circuit-based methods allow for stator currents that vary in the range from 0.6 to 1.5 p.u. [14–28];
- rotor short-circuit-based methods obtain 1 p.u. [14,18,30];
- and auxiliary converter-based techniques achieve a lower range of the stator-short circuit-based benchmark [31].

Therefore, the findings demonstrate that the proposed method achieves one of the lowest starting current values compared to the existing literature, near the lower range of stator short-circuit-based methods and comparable to converter-based techniques, as evidence of its suitability for DFIM starting. The initial magnetizing current provided by the

stator windings, fed from the grid, and the portion of magnetizing current provided by the converter during the process, are in the range of 0.4–0.6 p.u., well below the rated values.

The findings also highlight that the sinusoidal EMF induced on the rotor windings can be smoothly synchronized with the pulsed voltage applied by the power converter. The effects resemble grid synchronizations of synchronous machines, where the EMF inducted on the rotor windings is analogous to the grid voltage and the converter output is comparable to the synchronous machine output. However, here, voltage and frequency can be managed by the converter and have a pulsed characteristic, while voltage and frequency control under no-load conditions is performed, and a sinusoidal waveform is obtained, in synchronous machines. The quality of the synchronization is crucial for the smoothness of the method when the standstill synchronization is performed.

After synchronization, it is shown that the flux creation transient provided by the stator windings remains largely below the rated value. It is further demonstrated that the initial oscillatory currents at the initial stage of the acceleration, and the resulting oscillatory effects on torque, are an outcome of the mechanical characteristics of the machine and remain within tolerable limits. The soft acceleration is achieved with a gradual decrease in rotor frequency. In order to avoid current peaks during the acceleration, the rotor frequency reduction rate should be controlled to prevent the machine inertia from behaving similarly to a load. Under no-load conditions, the machine only draws magnetizing and accelerating currents throughout the acceleration process. The magnetizing current, which is initially drawn entirely from the stator, is progressively distributed between the stator and rotor. This distribution depends on the machine's characteristic impedances and follows the opposite evolution to the one shown in [32]. The accelerating current is supplied by the rotor side as the machine accelerates, enabling the desired slip. This balanced distribution of currents, coupled with the smooth synchronization and controlled acceleration, underscores the effectiveness and practicality of the proposed method for achieving reliable DFIM starting.

6.2. Analysis of Advantages and Limitations

As deduced from Section 2 and Table 1, the proposed method offers significant practical advantages over existing methods [12–32]. The high torsional stress on the rotor caused by opposite-phase synchronizations [12] is avoided. Moreover, additional bulky and costly power equipment, such as autotransformers and variable rotor resistances [13], or electronic converters [29,31], is not required. Furthermore, stator and rotor short-circuit-based methods [14–30] involve notable complexity and pose security risks due to the direct short-circuit maneuver. Also, these techniques require high-power commutation switches capable of withstanding short-circuit currents, and in the case of the rotor short-circuit, an increased converter power rating is necessary to bring the machine up to the rated speed by feeding the stator, all of which is avoided through the proposed approach.

In comparison with the previous standstill synchronization-based method proposed by the authors [32], performing standstill synchronization on the rotor side of the DFIM offers notable advantages, which will be analyzed in the following.

The main advantage lies in initially feeding the machine from the stator. This technique allows the entire initial magnetizing current to be drawn from the grid, instead of relying on the converter for this purpose, as in [32]. This reduces the electrical stress on the converter, thereby extending its operational lifespan. From the system design perspective, it lowers the converter's rating requirements, resulting in reduced overall system costs. While the method in [32] required an initial rotor current of approximately 1 p.u., the improvement proposed in this work reduces that requirement to 0.4 p.u., attained at the end of the acceleration stage, when a greater part of the magnetizing current is supplied through

the rotor circuit. This represents a 60% reduction in the stress applied to the converter, enhancing its longevity in operation, or alternatively, a 60% reduction in the converter's power converter rating requirement, leading to significant cost savings in system design.

Other benefits of the proposed method over the stator-side synchronization counterpart [32] include that synchronizations conducted on the lower-voltage side of the DFIM tend to be less abrupt than those on the opposite side. Moreover, by performing the synchronization on the rotor side, another important advantage is that the high-frequency commutation pulses due to PWM of the RSC present before synchronization in the method proposed in [32] are avoided, as the DFIM's stator windings are directly fed from the power system before synchronization, with sinusoidal currents and voltages. This results in lower electrical stress on the stator winding insulation than in the stator-side synchronization counterpart.

However, the most significant drawback of this method is the requirement for an additional switch, S1, while the stator-side synchronization counterpart [32] only relies on the main CB to carry out the starting process. Nevertheless, while if the synchronization is conducted on the stator side, the CB is subjected to high PWM stress, the S1 switch in the case of rotor-side synchronizations needs to withstand notably lower PWM stress, specifically, at r_t times lower voltage magnitude, which helps relieve the requirements on switch S1.

The presence of higher converter output voltages during the initial stage of the starting process, compared to the voltages applied by the converter in steady-state operation with low slip values, is another noteworthy drawback of the method. Finally, it should be noted that the starting speed is limited by the intended softness. In fact, the acceleration speed is inversely proportional to the converter frequency decrease during the process. The rotor frequency reduction rate should be moderated to prevent the machine inertia from behaving similarly to a load and thereby causing excessive current and torque peaks that can undermine the softness.

6.3. Influence of the Control Strategy

The proposed soft-starting method employs a scalar control strategy with constant V/Hz during the acceleration phase after synchronization, for illustrative purposes. This approach was selected for its simplicity and effectiveness in ensuring a smooth transition to the desired slip frequency while maintaining constant magnetic flux and avoiding saturation. Although scalar control is traditionally associated with steady-state analysis, it has been successfully implemented in the transient processes presented in this work. Both simulations and experimental results confirm that this control strategy adequately handles transient dynamics, resulting in low starting currents, minimized torque oscillations, and a seamless acceleration process. It is important to emphasize that the novelty of this work lies not in the specific control strategy employed during the transient phase but in the development of the rotor-side synchronization-based starting method. The method is compatible with various control strategies, including field-oriented control (FOC) or direct torque control (DTC), as long as they ensure smooth frequency and voltage transitions during the acceleration phase.

6.4. Influence of the Modulation Technique

The simulations and experiments presented in this work employed unipolar PWM modulation. This can be observed in the waveforms of the rotor voltage on the power converter side (Figures 7 and 11), which exhibit three distinct voltage levels. The choice of unipolar PWM was made to minimize harmonic distortion in the lower frequency range and reduce dv/dt stress on the machine windings, which is beneficial for long-term reliability

and insulation lifespan. However, it should be noted that the proposed synchronization and starting method is independent of the modulation strategy used, such as unipolar PWM, bipolar PWM, or space vector modulation (SVM). The synchronoscope, which aligns the fundamental harmonic components of the stator and rotor voltages, ensures that synchronization is governed by the first harmonic, making the method compatible with any modulation strategy. This flexibility further underscores the practicality of the proposed technique.

6.5. Influence of Machine Parameters

The simulation and experimental analyses presented in this work were conducted on two different DFIMs, each with unique design parameters and dynamic characteristics. Despite these distinctions, the results from both simulations and experiments exhibit consistent and comparable startup dynamics, including smooth acceleration, low starting currents, minimized torque oscillations, and successful synchronization using the proposed method. The observed differences between the machines primarily impact secondary characteristics, such as the attenuation of oscillations and the duration of transient regimes, which are governed by machine-specific factors, such as the rotor's moment of inertia and the RL circuit parameters. These variations underscore the robustness and adaptability of the starting method, which demonstrates consistent performance across machines with differing electrical and mechanical properties.

Particularly, in this work, the simulations and experiments were conducted using two distinct DFIMs, each with a specific stator-to-rotor voltage ratio (r_t), determined by their design characteristics. The simulation model employed a smaller DFIM with r_t = 10/1 [V/V], while the machine used for experimental testing had r_t = 2.10 [V/V], derived from its nameplate specifications. This ratio is a constant value determined by the winding configuration and voltage design of each machine, and it primarily affects the voltage requirements of the RSC, with higher r_t reducing converter costs by requiring lower rotor voltages, and higher rotor currents, for the same power. However, grid stability and power losses during starting are more closely related to the starting method than to the value of r_t. In the proposed method, with the magnetization performed from the stator side, issues related to high r_t values vanish.

6.6. Applicability to Higher Power Systems

The proposed soft-starting method demonstrates strong potential for application to higher-rated DFIMs (e.g., >1 MW), with its advantages likely becoming more pronounced in such systems. Larger machines typically require a smaller proportion of magnetizing current relative to their total current, leading to reduced relative losses and inrush currents during energization. In these cases, the smooth acceleration process inherent to the method further minimizes the grid impact by keeping the inrush currents within a tolerable range, typically between 0.2–0.4 p.u. Ensuring soft acceleration by moderating the rate of change of frequency imposed by the converter is even more important in machines with large inertia, in order to avoid excessive current peaks during the acceleration process. At the end of the start-up, when the machine reaches the desired speed under unloaded conditions, the injected currents stabilize as a combination of the magnetizing current and the current required to overcome mechanical losses, with final currents approaching 1 p.u. under nominal loaded conditions.

Moreover, scaling the method to larger machines introduces some practical challenges, such as the need for power converters with higher voltage and current ratings and the additional energy required to accelerate larger moments of inertia. These factors necessitate robust converter designs and precise control strategies to maintain smooth voltage and

frequency regulation during synchronization. Larger machines may also exhibit more pronounced mechanical resonances or longer transient durations, which would need careful handling to ensure optimal performance. Despite these considerations, the fundamental principles of the proposed method remain robust and adaptable, making it well suited for high-power applications.

7. Conclusions

This work presents an improved DFIM soft-starting method based on the synchronization to the power system at standstill conditions. The improved method relies on the synchronization performed on the rotor side. The stator of the DFIM is initially fed from the power system, while the rotor converter adapts the voltage and frequency to achieve the synchronization conditions. Once these conditions are met, the rotor breaker is closed. Finally, the rotor converter frequency is decreased, and consequently the machine is accelerated.

The method has been validated through both computer simulations and experimental tests. The method demonstrates several general advantages:

- Reduced complexity and cost: The need for additional components, such as auxiliary converters, autotransformers, or short-circuiting switches, is eliminated, making the system more straightforward and cost-effective.
- Enhanced grid stability: By minimizing inrush currents and avoiding voltage sags, the method supports the stability of power systems, particularly those with weaker configurations. The proposed technique achieves one of the lowest starting current levels among existing methods, comparable to or better than state-of-the-art solutions.
- Smooth startup: The results confirm that the proposed method ensures a seamless acceleration process with reduced transient currents and torque oscillations.

Specifically, compared to the previous method, based on stator-side synchronization at standstill conditions, the improved method presents remarkable advantages. The main benefit is that as the magnetizing current is provided by the grid, the electrical stress on the power converter is notably decreased. This enhances the durability and decreases the operational costs of the converter over time. Moreover, the power rating requirements for the converter can be significantly reduced. Additional benefits include smoother synchronization, reduced stress on stator windings insulation, and lower-voltage high-frequency commutation pulses affecting the switchgear.

The limitations of the method include the fact that the softness achieved is inversely proportional to the operational speed, the use of an additional switch on the rotor side, and the presence of higher converter output voltages during the initial stage of the process compared to the voltages applied by the converter in steady-state operation with low slip values.

The starting method has been assessed under free shaft conditions, which is the typical situation in variable-speed hydro pumped storage units. Future works may explore the integration of this method into large-scale hydropower systems, examining its performance under different operational conditions, including loaded start-ups.

Author Contributions: Conceptualization, K.M., J.M.G., J.A.S. and C.A.P.; methodology, K.M., J.M.G., J.A.S. and C.A.P.; software, K.M. and J.M.G.; validation, J.A.S. and C.A.P.; formal analysis, J.A.S.; investigation, K.M. and J.M.G.; resources, C.A.P.; data curation, K.M. and J.M.G.; writing—original draft preparation, K.M., J.M.G. and J.A.S.; writing—review and editing, K.M., J.M.G., J.A.S. and C.A.P.; visualization, K.M. and J.M.G.; supervision, C.A.P.; project administration, C.A.P.; funding acquisition, C.A.P. All authors have read and agreed to the published version of the manuscript.

Funding: This research was partially funded by Universidad Politécnica de Madrid, grant number RP2304330031.

Data Availability Statement: Datasets available on request from the authors.

Conflicts of Interest: The authors declare no conflicts of interest.

Nomenclature

$\Delta\varphi$	Phase difference
Δf	Frequency difference
ΔU	Voltage magnitude difference
C	DC bus capacitance
f_{grid}	Grid frequency
f_r	Converter-fed rotor frequency
f_s	Stator frequency
H	Inertia
I_r	Converter-fed rotor current
I_s	Stator current
J	Moment of inertia
L_m	Mutual inductance
L_r	Rotor inductance
$L_r{}'$	Rotor inductance referred to stator
L_s	Stator inductance
n	Mechanical rotor speed
p	Number of pole pairs
P	Real power
R_r	Rotor resistance
$R_r{}'$	Rotor resistance referred to stator
R_s	Stator resistance
r_t	Stator/rotor voltage ratio
R_{var}	Variable resistance
s	Slip
T_m	Mechanical torque
T_r	Mechanical counter-torque
t	Time
U_{DC}	DC bus voltage
U_{grid}	Grid voltage
U_r	Converter-fed rotor voltage
U_s	Stator voltage
X_m	Magnetizing reactance
X_r	Rotor leakage reactance
X_s	Stator leakage reactance
φ_r	Rotor phase angle
φ_s	Stator phase angle
Ψ_r	Rotor flux
Ψ_s	Stator flux
ω_0	Angular speed
ω_m	Mechanical rotor angular speed

Abbreviations

AC	Alternating current
AT	Autotransformer
CB	Circuit breaker
DC	Direct current
DFIM	Doubly fed induction machine
DTC	Direct torque control
EMF	Electromotive force
FOC	Field-oriented control
GSC	Grid-side converter
IGBT	Insulated-gate bipolar transistor
IK	Impact protection
IP	Ingress protection
PF	Power factor
PLL	Phase-locked loop
PWM	Pulse-width modulation
RMS	Root mean square
RSC	Rotor-side converter
SVM	Space vector modulation
V/Hz	Volts/hertz
VSC	Voltage source converter

References

1. Valavi, M.; Nysveen, A. Variable-Speed Operation of Hydropower Plants: A Look at the Past, Present, and Future. *IEEE Ind. Appl. Mag.* **2018**, *24*, 18–27. [CrossRef]
2. Donalek, P.J. Pumped Storage Hydro: Then and Now. *IEEE Power Energy Mag.* **2020**, *18*, 49–57. [CrossRef]
3. Mahfoud, R.J.; Alkayem, N.F.; Zhang, Y.; Zheng, Y.; Sun, Y.; Alhelou, H.H. Optimal Operation of Pumped Hydro Storage-Based Energy Systems: A Compendium of Current Challenges and Future Perspectives. *Renew. Sustain. Energy Rev.* **2023**, *178*, 113267. [CrossRef]
4. Zhou, Y.; Zhu, Y.; Luo, Q.; Wei, Y.; Mei, Y.; Chang, F.-J. Optimizing Pumped-Storage Power Station Operation for Boosting Power Grid Absorbability to Renewable Energy. *Energy Convers. Manag.* **2024**, *299*, 117827. [CrossRef]
5. Xu, M.; Wu, D.; Wang, D.; Huang, B.; Desomber, K.; Fu, T.; Weimar, M. Optimizing Pumped Storage Hydropower for Multiple Grid Services. *J. Energy Storage* **2022**, *51*, 104440.
6. Shi, L.; Lao, W.; Wu, F.; Zheng, T.; Lee, K.Y. Frequency Regulation Control and Parameter Optimization of Doubly-Fed Induction Machine Pumped Storage Hydro Unit. *IEEE Access* **2022**, *10*, 102586–102598. [CrossRef]
7. Reddy, B.K.; Ayyagari, K.S.; Kumar, Y.P.; Giri, N.C.; Rajgopal, P.V.; Fotis, G.; Mladenov, V. Experimental Benchmarking of Existing Offline Parameter Estimation Methods for Induction Motor Vector Control. *Technologies* **2024**, *12*, 123. [CrossRef]
8. Alizadeh Bidgoli, M.; Yang, W.; Ahmadian, A. DFIM versus Synchronous Machine for Variable Speed Pumped Storage Hydropower Plants: A Comparative Evaluation of Technical Performance. *Renew. Energy* **2020**, *159*, 72–86. [CrossRef]
9. Yaramasu, V.; Wu, B.; Sen, P.C.; Kouro, S.; Narimani, M. High-Power Wind Energy Conversion Systems: State-of-the-Art and Emerging Technologies. *Proc. IEEE* **2015**, *103*, 740–788. [CrossRef]
10. *IEEE Std 1010-2022 (Revision of IEEE Std 1010-2006)*; IEEE Guide for Control of Hydroelectric Power Plants. IEEE: New York, NY, USA, 2023; pp. 1–95.
11. Tiwari, R.; Nilsen, R.; Mo, O. Control Strategies for Variable Speed Operation of Pumped Storage Plants with Full-Size Converter Fed Synchronous Machines. In Proceedings of the 2021 IEEE Energy Conversion Congress and Exposition (ECCE), Vancouver, BC, Canada, 10–14 October 2021; pp. 61–68.
12. Hamouda, R.M.; Alolah, A.I.; Badr, M.A.; Abdel-Halim, M.A. A Comparative Study on the Starting Methods of Three Phase Wound-Rotor Induction Motors. I. *IEEE Trans. Energy Convers.* **1999**, *14*, 918–922. [CrossRef]
13. Zhang, Y.; Ooi, B.T. Adapting DFIGs for Doubly-Fed Induction Motors Operation. In Proceedings of the 2012 IEEE Power and Energy Society General Meeting, San Diego, CA, USA, 22–26 July 2012; pp. 1–8.
14. Yuan, X.; Chai, J.; Li, Y. A Converter-Based Starting Method and Speed Control of Doubly Fed Induction Machine With Centrifugal Loads. *IEEE Trans. Ind. Appl.* **2011**, *47*, 1409–1418. [CrossRef]
15. Joseph, A.; Selvaraj, R.; Chelliah, T.R.; Sarma, S.V.A. Starting and Braking of a Large Variable Speed Hydrogenerating Unit Subjected to Converter and Sensor Faults. *IEEE Trans. Ind. Appl.* **2018**, *54*, 3372–3382. [CrossRef]

16. Joseph, A.; Desingu, K.; Semwal, R.R.; Chelliah, T.R.; Khare, D. Dynamic Performance of Pumping Mode of 250 MW Variable Speed Hydro-Generating Unit Subjected to Power and Control Circuit Faults. *IEEE Trans. Energy Convers.* **2018**, *33*, 430–441. [CrossRef]
17. Anto, J.; Chelliah, T.R. Starting Performance of Doubly Fed Induction Machine Drive Serving Pumped Storage Plants Subjected to Faults in Power and Control Circuits. In Proceedings of the 2016 IEEE 1st International Conference on Power Electronics, Intelligent Control and Energy Systems (ICPEICES), Delhi, India, 4–6 July 2016; pp. 1–7.
18. Saiju, R.; Koutnik, J.; Krueger, K. Dynamic Analysis of Start-Up Strategies of AC Excited Double Fed Induction Machine for Pumped Storage Power Plant. In Proceedings of the 2009 13th European Conference on Power Electronics and Applications, Barcelona, Spain, 8–10 September 2009; pp. 1–8.
19. Pannatier, Y.; Kawkabani, B.; Nicolet, C.; Schwery, A.; Simond, J.-J. Optimization of the Start-Up Time of a Variable Speed Pump-Turbine Unit in Pumping Mode. In Proceedings of the 2012 XXth International Conference on Electrical Machines, Marseille, France, 2–5 September 2012; pp. 2126–2132.
20. Pannatier, Y.; Kawkabani, B.; Nicolet, C.; Schwery, A.; Simond, J.-J. Start-Up and Synchronization of a Variable Speed Pump-Turbine Unit in Pumping Mode. In Proceedings of the XIX International Conference on Electrical Machines—ICEM 2010, Rome, Italy, 6–8 September 2010; pp. 1–6.
21. Li, D.; Gong, G.; Lv, J.; Jiang, X.; He, R. An Overall Control of Doubly Fed Variable Speed Pumped Storage Unit in Pumping Mode. In Proceedings of the 2020 IEEE 4th Conference on Energy Internet and Energy System Integration, Wuhan, China, 30 October–1 November 2020; pp. 3709–3714.
22. Gong, G.; Lv, J.; Jiang, X.; Sun, X. Grid-Connection Control of Doubly Fed Variable Speed Pumped Storage Unit. In Proceedings of the 2021 5th International Conference on Green Energy and Applications (ICGEA), Singapore, 6–8 March 2021; pp. 52–57.
23. Zhu, K.; Ruan, L. Self-Starting Control Strategy of Variable Speed Pumped Storage Unit Based on Adaptive Full Order State Observer. *Meas. Control* **2023**, *56*, 630–637. [CrossRef]
24. Yang, J.; Zhang, F.; Hou, K.; Zeng, X. Study on Self-Starting Technology of Pumped Storage Unit Considering Iron Loss of Doubled Fed Motor. In Proceedings of the 2024 IEEE 7th International Electrical and Energy Conference (CIEEC), Harbin, China, 14–16 June 2024; pp. 2641–2646.
25. Ji, L.; Shao, Y.; Sun, J.; Shi, L. Research on Self-Starting Strategy of Variable Speed Pumped Storage Units Based on Model Predictive Control. *J. Eng.* **2017**, *2017*, 984–989. [CrossRef]
26. Maendly, T.; Hodder, A.; Kawkabani, B. Start-Up of a Varspeed Group in Pump Mode: Practical Implementations and Tests. In Proceedings of the 2016 XXII International Conference on Electrical Machines (ICEM), Lausanne, Switzerland, 4–7 September 2016; pp. 1201–1207.
27. Singh, R.R.; Baranidharan, M.; Subramaniam, U.; Bhaskar, M.S.; Rangarajan, S.S.; Abdelsalam, H.A.; Collins, E.R.; Senjyu, T. An Energy-Efficient Start-Up Strategy for Large Variable Speed Hydro Pump Turbine Equipped with Doubly Fed Asynchronous Machine. *Energies* **2022**, *15*, 3138. [CrossRef]
28. Singh, R.R.; Chelliah, T.R. Energy Saving Start-Up Strategy of Pumped Storage Power Plant Equipped with Doubly-Fed Asynchronous Machine. In Proceedings of the 2016 IEEE 1st International Conference on Power Electronics, Intelligent Control and Energy Systems (ICPEICES), Delhi, India, 4–6 July 2016; pp. 1–6.
29. Pérez-Díaz, J.I.; Cavazzini, G.; Blázquez, F.; Platero, C.; Fraile-Ardanuy, J.; Sánchez, J.A.; Chazarra, M. Technical Report, Mechanical Storage Subprogramme, Joint Programme on Energy Storage. In *Technological Developments for Pumped-Hydro Energy Storage*; European Energy Research Alliance: Brussels, Belgium, 2014.
30. Narayanasamy, M.; Sukhi, Y. Rotor Short-Circuited Start-Up Strategy for a Doubly Fed Induction Machine-Fed Large-Rated Variable-Speed Pumped Storage Unit Operating in Pumping Mode. *J. Power Electron.* **2023**, *23*, 1733–1744. [CrossRef]
31. Malathy, N.; Sukhi, Y. Improved Start-Up Strategy for a Doubly Fed Induction Machine Fed Large Rated Variable Speed Pumped Storage Unit in Pumping Mode Operation. *Electr. Eng.* **2023**, *106*, 615–629. [CrossRef]
32. Guerrero, J.M.; Mahtani, K.; Aranzabal, I.; Gómez-Cornejo, J.; Sánchez, J.A.; Platero, C.A. A Soft Start Method for Doubly Fed Induction Machines Based on Synchronization with the Power System at Standstill Conditions. *Machines* **2024**, *12*, 847. [CrossRef]
33. Kovács, P.K. Transient Phenomena in Electrical Machines. In *Studies in Electrical and Electronic Engineering*; Elsevier: Amsterdam, The Netherlands, 1984.